Journal of Applied Mechanical Engineering
ISSN: 2168-9873

Surya et al., J Appl Mech Eng 2017, 6:3
DOI: 10.4172/2168-9873.1000263

Research Article Open Access

CFD Simulation of Ejector in Steam Jet Refrigeration

Surya SD[1], Vasu TA[2], Raghavan KS[1]* and Murthy Chavali[3]

[1]Department of Mechanical Engineering, National Chung Cheng University, Taiwan
[2]Department of Mechanical Engineering, Vignan's University, Guntur, Andhra Pradesh, India
[3]Divisions of Chemistry, Department of Sciences and Humanities, Vignan's University, Guntur, Andhra Pradesh, India

Abstract

In this study CFD technique was employed to investigate the effect of divergent angle of primary nozzle, NXP (NXP = Distance between the nozzle exit to mixing chamber inlet) and throat of the ejector on the performance of ejector using the steam jet refrigeration cycle. In all these cases, only one fixed mixing chamber with different divergent primary nozzle, NXP and throat of an ejector was investigated numerically using the commercial CFD package, the effect of primary fluid pressure mass flow rate and mach numbers were observed and analyzed. The velocity contour lines were used to explain the happening of process inside the ejector it was found that the throat diameter, NXP and diverging angle of primary nozzle plays a crucial role in the steam jet refrigeration.

Keywords: Ejector; Steam jet

Nomenclature: COP: Coefficient of Performance; NXP: Nozzle Exit Position (mm); P: Absolute Pressure (bar, mbar); T: Temperature (°C); Rm: Entrainment ratio of an Ejector; h: Specific Enthalpy (kJ/kg); A: Cross-Section Area (m^2); M: Mach Number; m: Mass Flow Rate (kg/min, kg/hour); k: Specific Heat Ratio (1.32 for Water Vapor); d: Primary Nozzle's Throat Diameter (mm); D: Primary Nozzle Exit's Diameter (mm)

Subscripts: cri: Condition at critical condenser pressure; boiler: Condition at boiler pressure; cond: Condition at condenser pressure; evap: Condition at evaporator pressure; g-boiler: Saturated vapor at the boiler temperature; g-evap: Saturated vapor at the evaporator temperature; f-con: Saturated liquid at the condenser temperature; exit: Primary nozzle's exit plane; throat: Primary nozzle's throat; k-u-sst: Showing the results of the turbulence viscosity k-u-sst; k-ε: Showing the results of the turbulence viscosity realizable k-ε

Introduction

A steam jet refrigeration framework is an intriguing heat-powered. Refrigeration framework because of its natural inviting operating. Character. It camwood change over waste high temperature (low-grade warm energy). That is dismisses from numerous mechanical methods with handy refrigeration. Thereby diminishing the electrical vitality utilization of the. Air-conditioning framework. In turn preference, may be that water, the majority. Ecological inviting substance, might be utilized Likewise those working liquid. In the framework. Through as far back as decades, a number analysts need attempted. On move forward those steam jet refrigeration frameworks. A few analysts. Investigated the impact for working states on the framework [1-6].

Figure 1 displays a schematic see of a steam ejector refrigeration. Framework. Those high points Furthermore high engineering immersed steam may be. Generated in the heater Also it will be utilized Concerning illustration those essential liquid for the. Ejector. The ejector draws low weight water vapor starting with those. Evaporator Likewise its optional liquid. This reason the water on dissipate, at low weight Furthermore prepare the refrigeration impact. That ejector. Discharges its debilitate of the condenser the place it may be condensed In the. Encompassing temperature. Some of the fluid will be pumped again of the. Heater same time the leftover portion is came back of the evaporator. Execution of the steam jet refrigeration may be characterized as far as the. Coefficient about execution (COP):. Cop

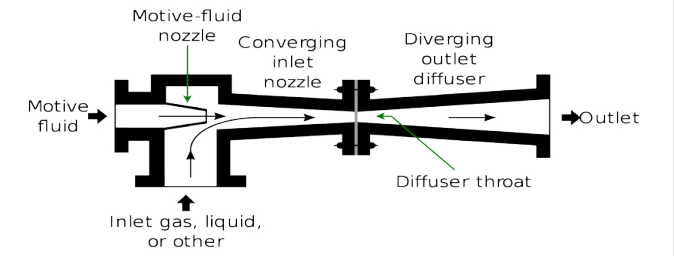

Figure 1: Schematic diagram of ejector.

¼ Rm$. Hg_{evap} hf_{con}. Hg_{boiler} and hf_{con}. The place Rm is characterized likewise those entrainment proportion of the ejector:. Rm ¼ impostor stream of the auxiliary liquid. Impostor stream of the grade liquid. Since the enthalpy transform In the heater will be very little separate. From the enthalpy transform In the evaporator, it might be expected that $COPz_{Rm}$.

Computational liquid Progress (CFD) camwood make used to illustrate those. Wonder inside the ejector. CFD's comes about accessible in the writing were discovered on consent great for test [7-15]. Qualities. Therefore, those CFD system could a chance to be used to faultlessly. Anticipate those execution of the steam jet refrigeration framework, impacts of the essential nozzle's [4]. Geometries and the working states on the ejector execution. Were broke down tentatively. The steam ejectors Concerning illustration indicated as shown in Figure 2 were tried for eight distinctive elementary nozzles. At. Extents for essential nozzles need aid exhibited for Table 1. The heater. Temperatures were differed in the extent about 110°C to 150°C. Those. Evaporator temperature might have been settled at 7.5°C. The tests

***Corresponding author:** Raghavan KS, Department of Mechanical Engineering, National Chung Cheng University, Taiwan, Tel: +886-422840433; E-mail: aradhyulatirumalavasu@gmail.com

Received March 14, 2017; **Accepted** April 01, 2017; **Published** April 06, 2017

Citation: Surya SD, Vasu TA, Raghavan KS, Chavali M (2017) CFD Simulation of Ejector in Steam Jet Refrigeration. J Appl Mech Eng 6: 263. doi: 10.4172/2168-9873.1000263

indicated that those throat breadth and the zone proportion of the essential spout. Determinedly impact those framework execution.

In this study, a CFD business programming package, familiar 6.3, Might have been used to examine those outcomes of the past consider [4] which. Were got tentatively. The feasible k-ε Furthermore k-u-sst. Turbulence viscosity models were chose to legislate the turbulence [16-18]. The reproduced effects starting with both CFD models. (entrainment proportion Furthermore incredulous condenser pressure) were compared. With the test brings about request to guarantee that it camwood make utilized. Faultlessly. The effects utilizing the k-u-sst turbulence viscosity model. Gave that's only the tip of the iceberg exact comes about over the feasible k-ε model. The. Mach number shape lines of the stream inside those ejector were. Exhibited graphically Also were used to dissect the stream conduct technique. Inside the steam ejector. For the utilization of the CFD technique,. A better Comprehension of the stream conduct inside the ejector, which will be specifically identified with that ejector's performance, was gotten?

Ejector operation

As appeared in Figure 1, a run of the mill ejector is made out of an essential spout, a blending chamber and a diffuser. The working rule for the ejector is straight forward. An ejector has two deltas: one to concede the rationale liquid stream at high weight liquid and other to concede the optional liquid stream at low weight. The thought process liquid enters the focalizing wandering spout where, the weight vitality of the intention liquid is changed over to active vitality, thus, at the exit of the spout, the liquid speed gets to be distinctly supersonic and a low weight zone is made. This low weight made empowers the optional liquid to be entrained or pumped through other channel.

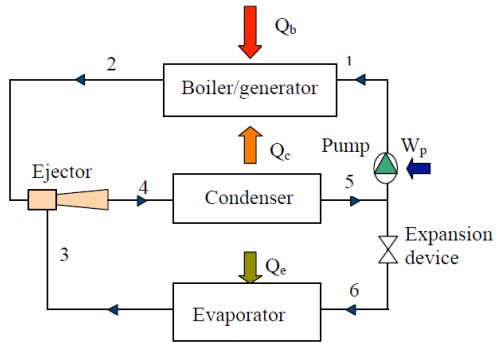

Figure 2: Schematic diagram of ejector refrigeration cycle.

Parameter	Entrainment Ratio
Increasing the divergent angle of primary nozzle	Decreases
Throat diameter of ejector is decreases	Decreases
NXP is increases	Increases

Table 1: Extents for essential nozzles.

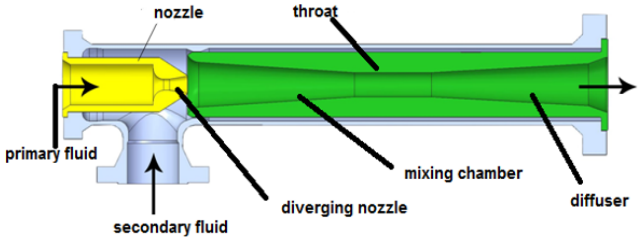

Figure 3: Ejector.

The entrained vapor stream accordingly blends with rationale liquid stream while they travel through the uniting area of the ejector, consequently, expanding weight at cost of dynamic vitality. The intention liquid backs off and the entrained stream accelerates and, sooner or later downstream the blending chamber, the blended stream achieves the speed of sound. A stationary stun wave is created in this way brings about a sharp ascent in outright weight. The stun wave in the diffuser throat moves the speed of blended stream from supersonic to sub-sonic. At that point, in the veering segment the expanding cross sectional region builds the weight to the detriment of active vitality. The net outcome, being an expansion of the outright weight of the blend on release to a few circumstances the weight at which optional liquid entered the ejector bay.

Ejector refrigeration system

A simple ejector refrigeration system consists of the following equipment:

i) Evaporator ii) Condenser iii) Boiler/Generator iv) Ejector v) Pump vi) Expansion Device.

Alluding to the fundamental ejector refrigeration cycle in Figure 2, the ejector refrigeration framework is made out of two sub cycles, the power sub-cycle and the refrigeration sub-cycle. In the power sub-cycle, second rate warm, Qb, is provided to evaporator or generator to vanish high weight fluid refrigerant (Process 1-2). At state point 2, the high weight vapor produced, known as the thought process liquid, enters the ejector and grows through the meeting veering spout making a low weight zone. This diminishment in weight entrains vapor from the evaporator, known as the optional liquid, at point 3. The entrained vapor stream accordingly blends with thought process liquid stream before entering the diffuser, while joined stream travels through the diffuser, the stream decelerates and weight recuperation happens. The consolidated liquid then streams to the condenser where it is dense dismissing warmth to the earth, Qc. At the condenser outlet the liquid stream is isolated into two sections at point 5, one segment is then pumped to the kettle for the culmination of the power cycle. The other bit is extended through a development gadget and enters the evaporator of the refrigeration sub-cycle at point 6. The refrigerant assimilates dormant warmth of vaporization producing a refrigeration effect, *Qe*, and the resulting vapor is then entrained into the ejector at point 3.

$$COP = \frac{R_M hg\_evap - hf\_con}{hg\_boiler - hf\_con}$$

Since the enthalpy change in the evaporator is not much different in the it is assumed to be COP=R_m

Computational fluid dynamics is used to explain the phenomenon inside the ejector. CFD results can predict accurately the performance of ejector. Ansys 16.0 is used to analyzing the results The realizable k-ε and k-omega-sst turbulence viscosity models were selected to govern the turbulence. after reaching the 140°c k omega sst model cannot predict accurately the flow inside the ejector. Therefore k-omega-sst model is used as turbulence models in all the analysis cases.

Results and Discussion

CFD Setup

The use of CFD technique was divided into two main parts one is creating the physical model and another is used solve the set of

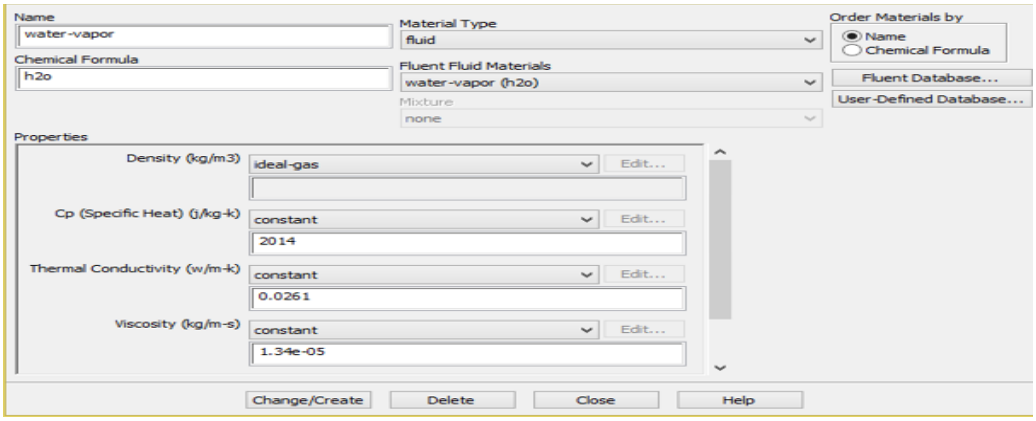

Figure 4: Working.

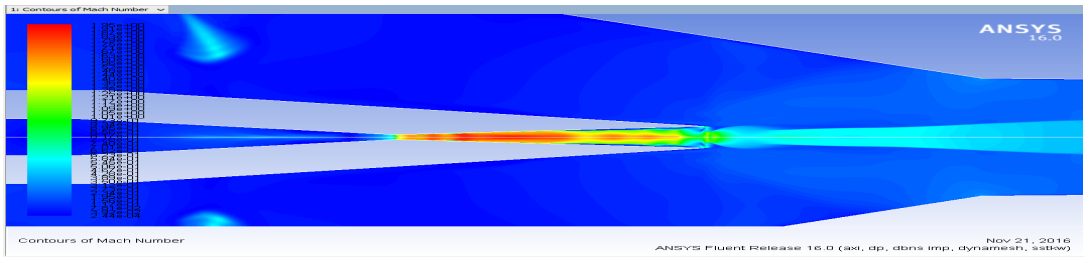

Figure 5: Velocity contour when divergent angle= 5°.

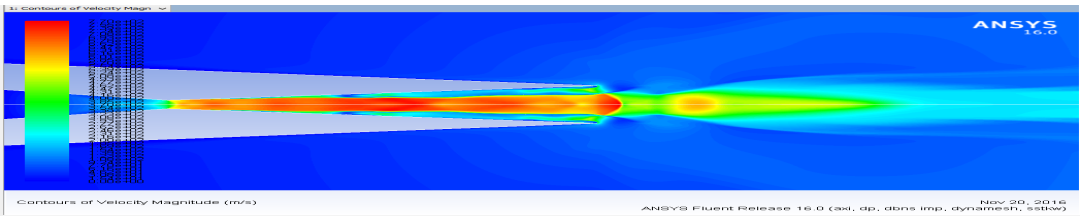

Figure 6: Velocity contour when divergent angle = 7.5°.

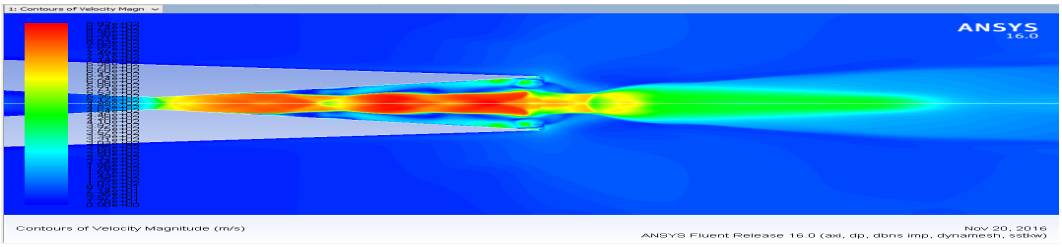

Figure 7: Velocity contour when divergent angle = 10°.

mathematical equations. Physical model and solving the mathematical equations were used by the Ansys workbench the dimensions of the physical model are explained in the Table 1. The gird elements were initially created in the form of quadrilateral of 140000 elements later it was increased to 180000 elements. This was ensure that the simulation results were independent from the number of grid elements (Figure 3). In this present work, the density-based implicit solver was selected to solve the governing equations which have been proven to be suitable for a supersonic flow field and the flow was set based on steady-state. The convective terms were discredited with a second order upwind scheme.

Working fluid properties

The velocity contour lines obtained from the CFD simulation are presented in the Figures 4-7 the boiler pressure was set to 476200 Pa, the pressure was set to 1002 pa and condenser pressure was set to 3000 Pa the nozzle throat diameter was set to 1 mm. Boiler pressure is named as primary pressure and evaporator pressure is set as secondary pressure. When the primary pressure enters into the primary nozzle at the throat the mach number is unity and therefore the flow is choked such that if any change happens in the downstream condition that will not be effect the upstream conditions. At the primary nozzle exit jet the

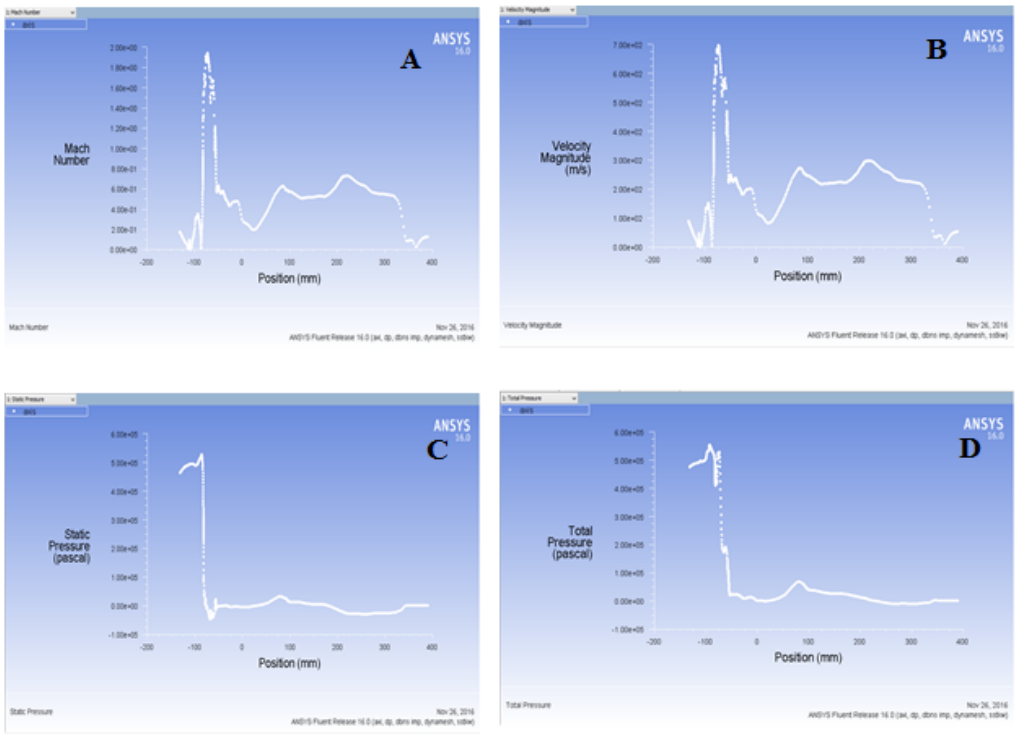

Figure 8: Mach number static pressure stagnation pressure velocity variations along the ejector when divergent angle=5°. (A) Mach number along the ejector (B) Static pressure variation along the ejector (C) Velocity variation along the ejector (D) Stagnation pressure variation along the ejector.

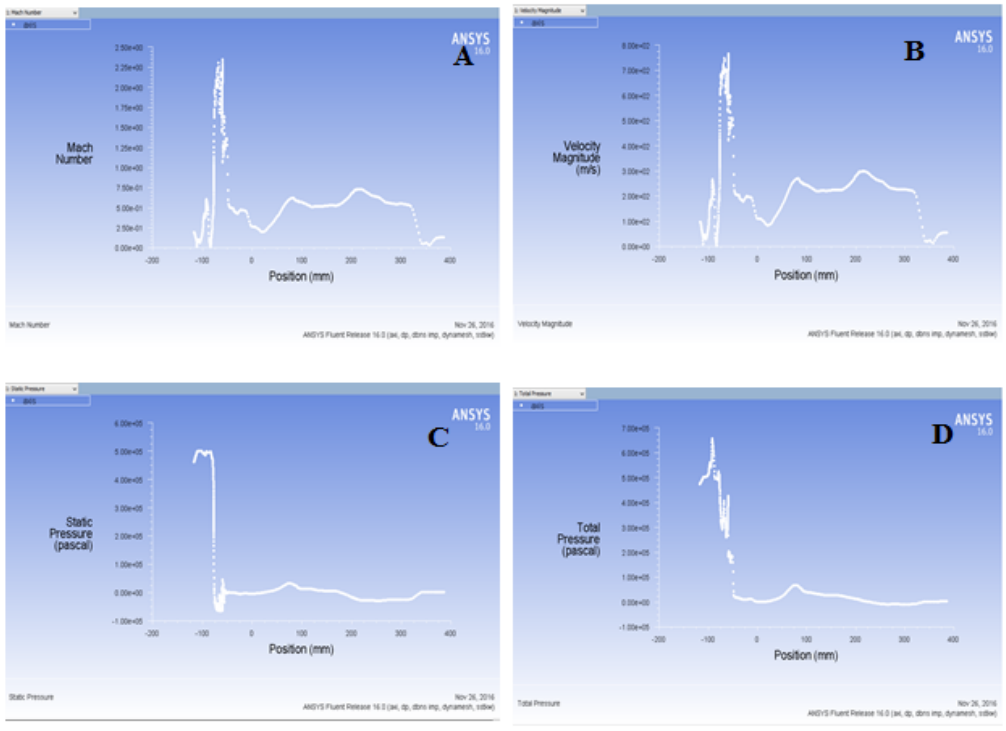

Figure 9: Mach number static pressure stagnation pressure velocity variations along the ejector when divergent angle=7.5°. (A) Mach number along the ejector (B) Static pressure variation along the ejector (C) Velocity variation along the ejector (D) Stagnation pressure variation along the ejector.

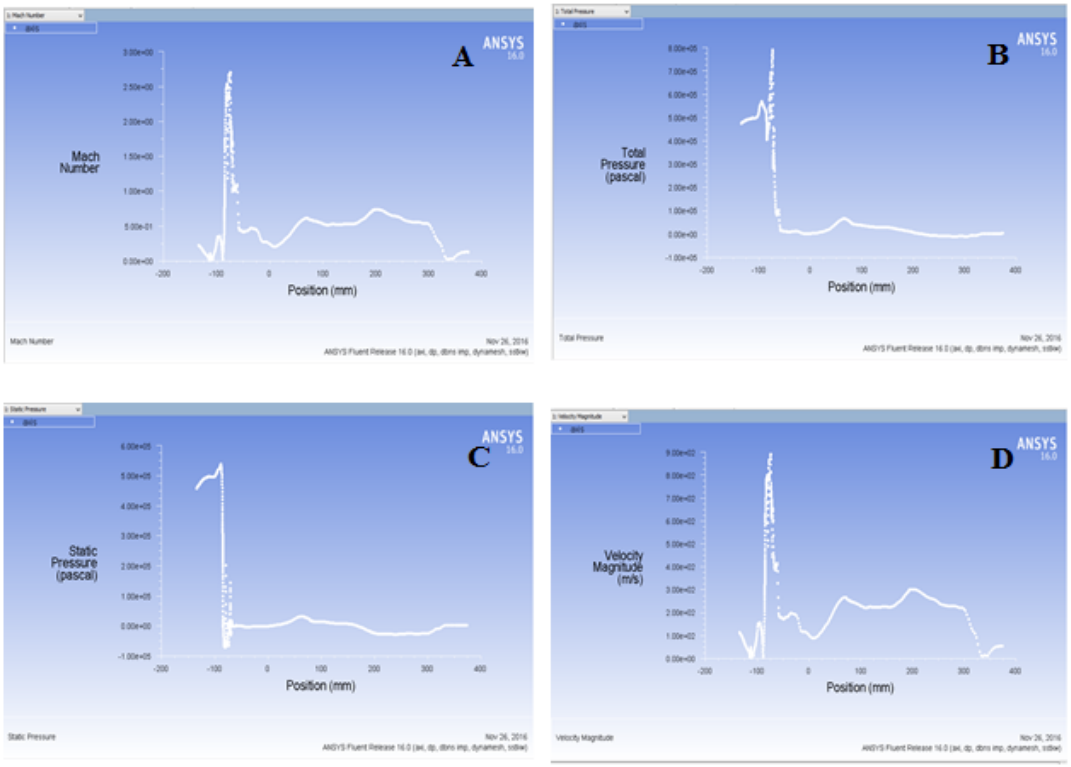

Figure 10: Mach number static pressure stagnation pressure velocity variations along the ejector when divergent angle=10°. A) Mach number along the ejector B) Static pressure variation along the ejector C) Velocity variation along the ejector D) Stagnation pressure variation along the ejector.

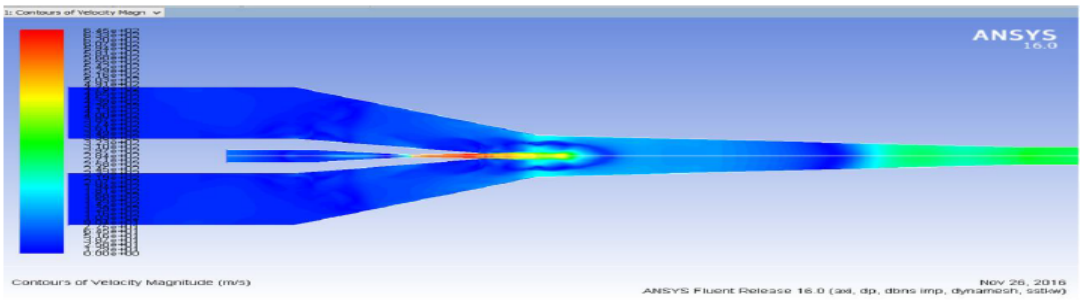

Figure 11: Throat inlet diameter = 10 mm.

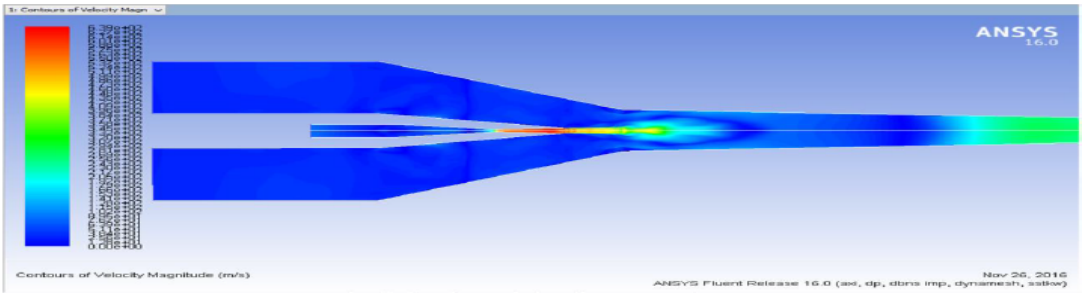

Figure 12: Throat inlet diameter = 15 mm.

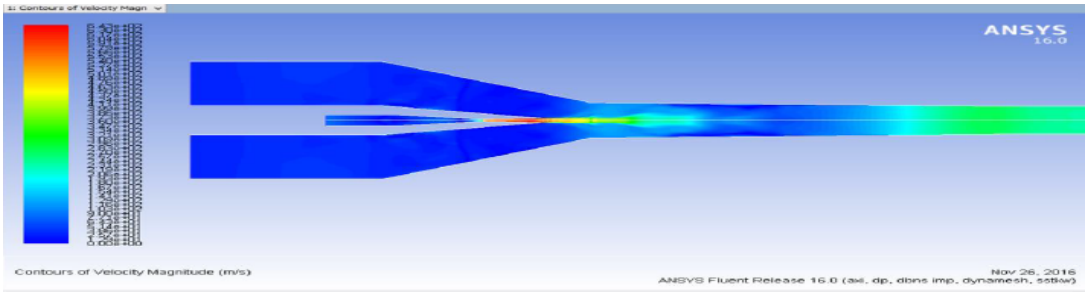

Figure 13: Throat inlet diameter =19 mm.

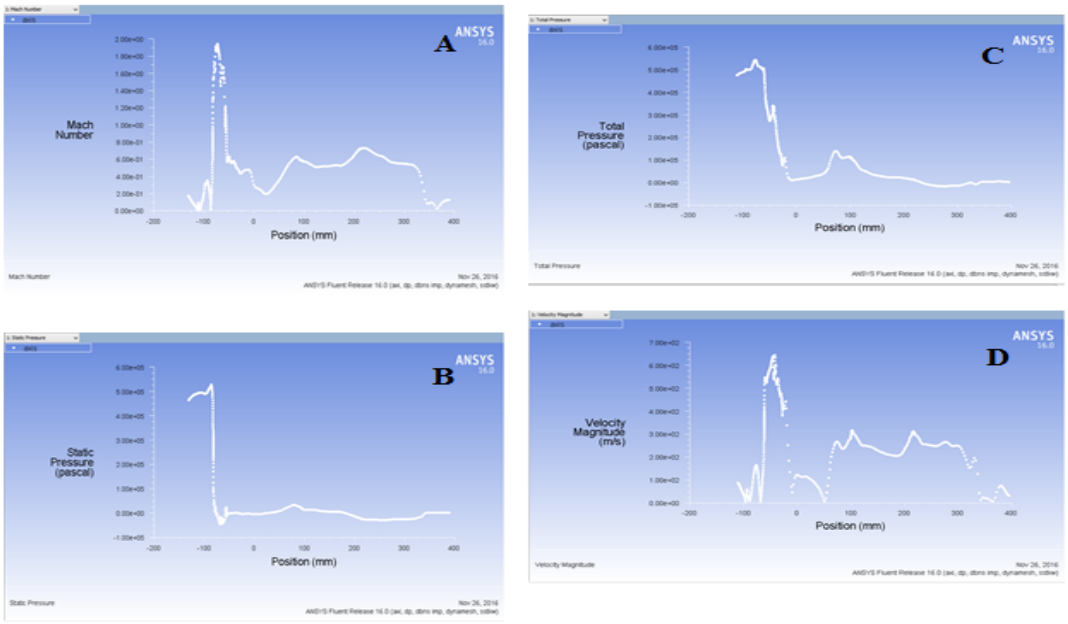

Figure 14: When all the dimensions and boundary conditions make to constant the Throat of the ejector was taken as 10 mm. A) Mach number variation along the ejector B) Static pressure variation along the ejector C) Stagnation pressure variation along the ejector D) Velocity variation along the ejector.

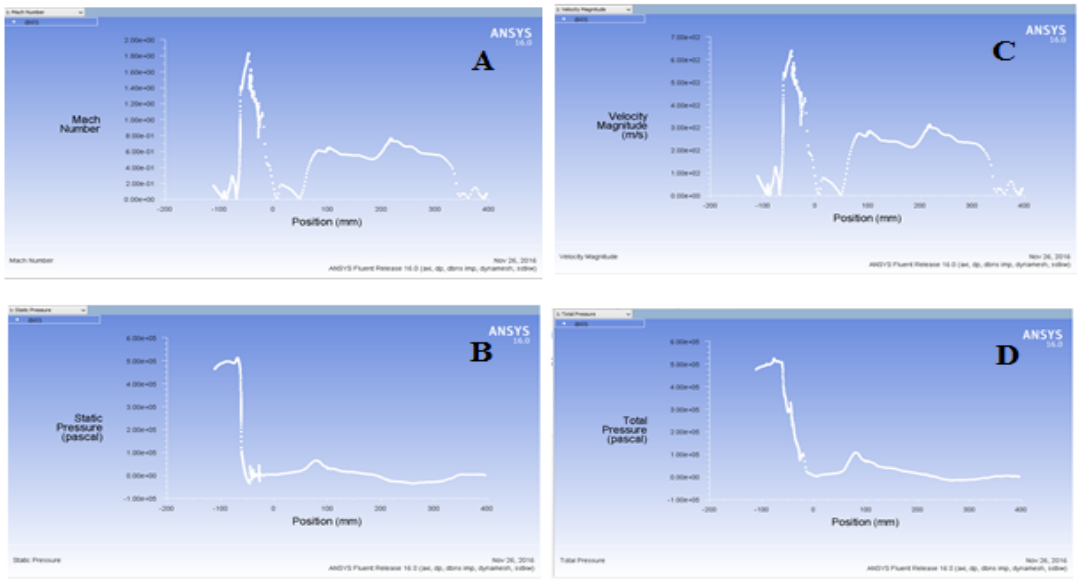

Figure 15: When all the dimensions and boundary conditions make to constant the Throat of the ejector was taken as 15 mm. A) Mach number variation along the ejector B) Static pressure variation along the ejector C) Velocity variation along the ejector D) Stagnation pressure variation along the ejector.

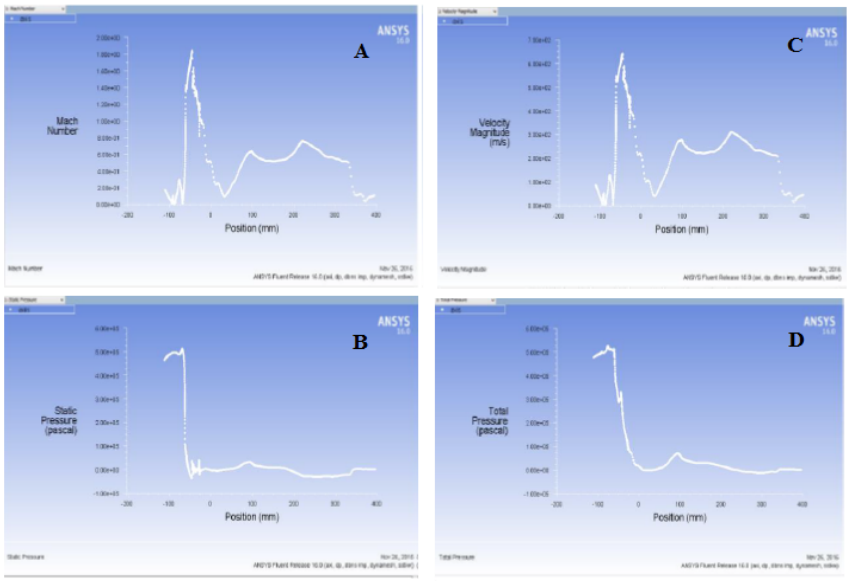

Figure 16: When all the dimensions and boundary conditions make to constant the Throat of the ejector was taken as 19 mm. A) Mach number variation along the ejector B) Static pressure variation along the ejector C) Velocity variation along the ejector D) Stagnation pressure variation along the ejector.

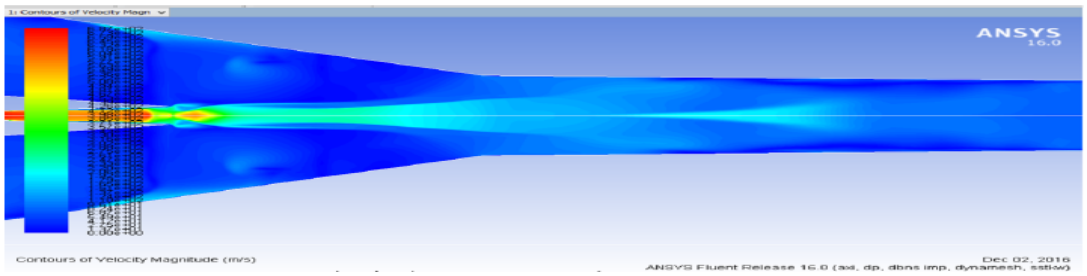

Figure 17: Velocity contours when NXP = 43.

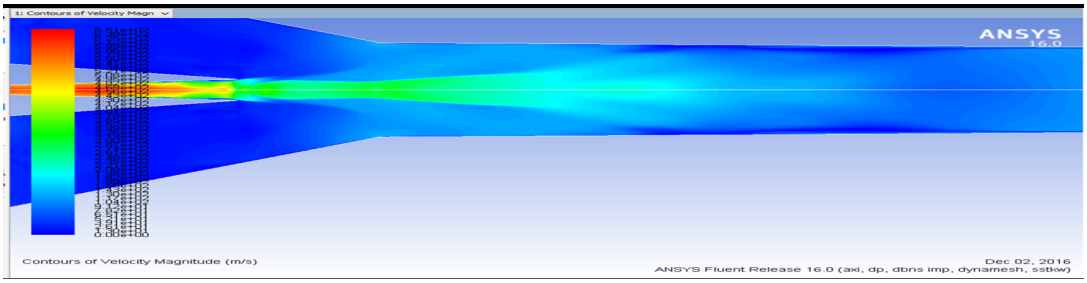

Figure 18: Velocity contours when NXP = 23.

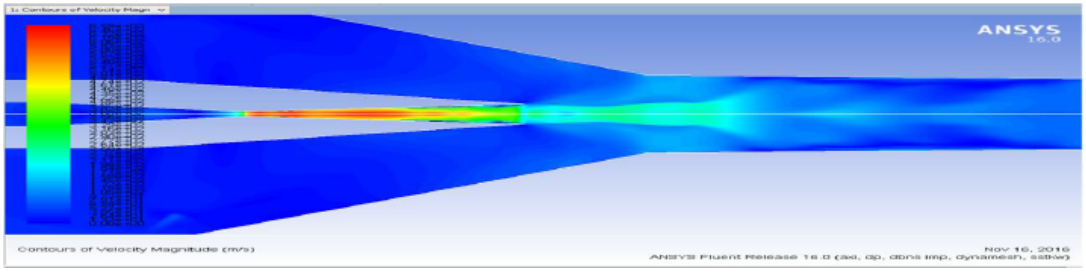

Figure 19: Velocity contours when NXP = 15.635.

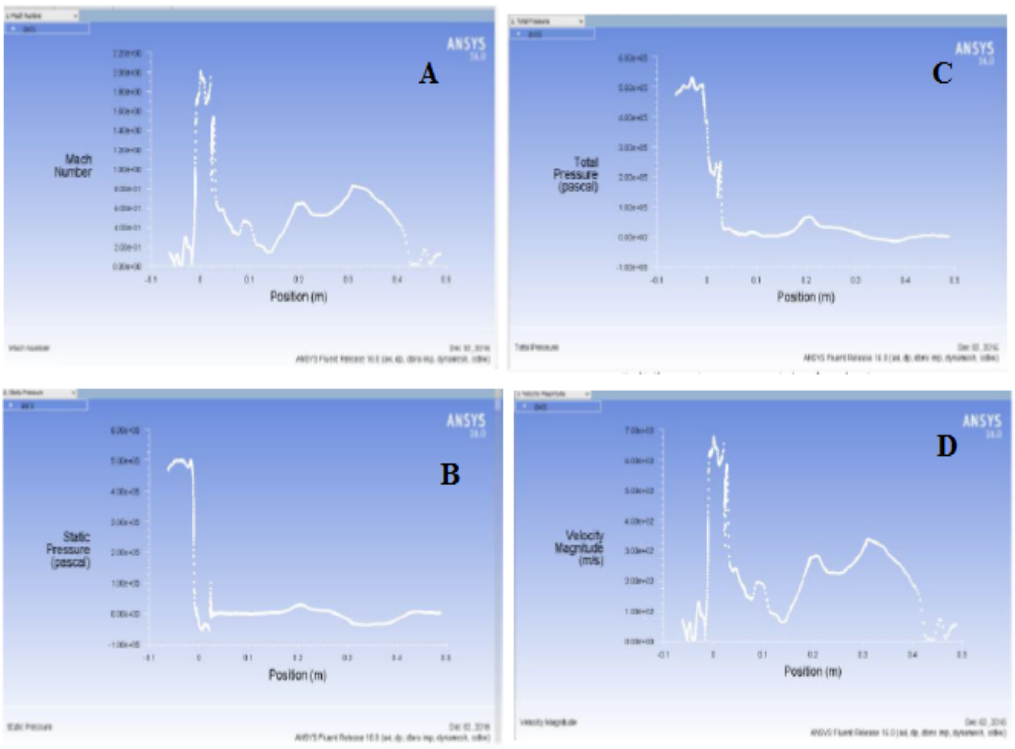

Figure 20: Velocity, Mach number, static pressure, total pressure plots along the axis of ejector when NXP = 43 mm. A) Mach number variation along the ejector B) Static pressure variation along the ejector C) Stagnation pressure variation along the ejector D) Velocity variation along the ejector.

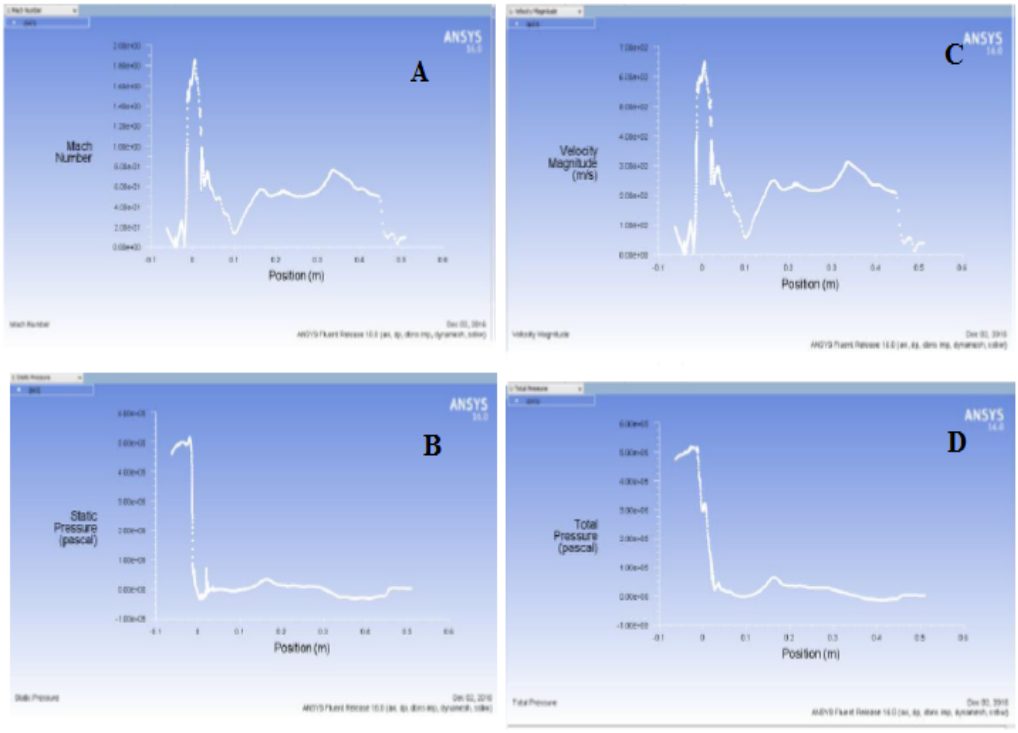

Figure 21: Velocity, Mach number, static pressure, total pressure plots along the axis of ejector when NXP = 23 mm. A) Mach number variation along the ejector B) Static pressure variation along the ejector C) Stagnation pressure variation along the ejector D) Velocity variation along the ejector.

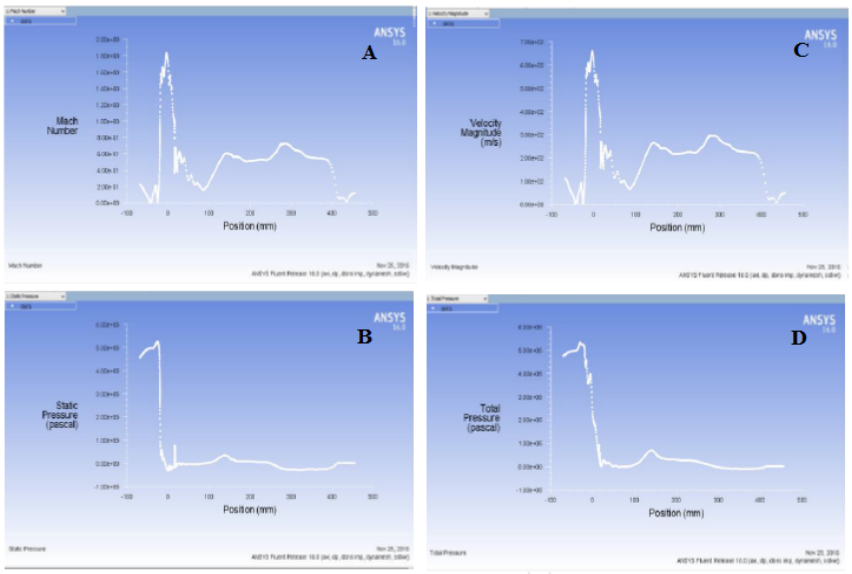

Figure 22: Mach number velocity static pressure and total pressure plots along the ejector when NXP=15.635 mm. A) Mach number variation along the ejector B) Static pressure variation along the ejector C) Velocity variation along the ejector D) Stagnation pressure variation along the ejector.

primary fluid leaves the pressure with supersonic stream which flows under free boundary conditions this leads the nozzle exit pressure leads to either under expanded wave or over expanded wave with converging angles or diverging angles. The expansion angle, converging duct and the effective area decides the entrainment ratio (Figures 8-10).

CFD results and discussions

Effect of divergent angle on the entrainment ratio: To launch this effect area ratio 20:1 is used with boiler pressure of 476200 Pa, the evaporator pressure is 1002 pa with condenser pressure of 3000 pa. the velocity contours explain the flowing phenomenon inside the ejector, when the divergent angle is increase an expanded wave is appearing in the mixing chamber is formed with larger expansion angles since the primary jet flows with a higher momentum, in this case a narrow converging duct and a smaller effective area are simultaneously produced therefore less amount of secondary fluid is entrained into the mixing chamber (Figures 11-13).

Effect of entrainment ratio on the variation of diameter of throat of ejector: To establish this effect the parameters are used by the ratio of nozzle is taken by 5:1. Throat of the ejector = 1.4 mm; Nozzle exit position = 15.635 mm; Mixing chamber inlet diameter = 24mm; Mixing chamber length = 130 mm; Length of throat of the ejector = 114 mm; Length of the diffuser = 180 mm; Diameter of diffuser = 40 mm; Boundary conditions boiler pressure inlet = 476200 Pa; Condenser pressure outlet = 3000 pa; Evaporator pressure inlet = 1002 pa.

The velocity contours are presented to explain this phenomenon It was seen that whenever the diameter of throat is decreases the entrainment ratio also decreases. Because the mixture of primary fluid and secondary fluid will not accelerate to pass through the throat so that incoming secondary mass flow rate to the mixing chamber is reduced (Figures 14-18).

Variation of entrainment ratio with respect to NXP

To establish this effect area ratio is of nozzle was taken as 20:1 and the mixing chamber length is 130 mm having the diameter of 24 mm throat having the length of 118 mm having the diameter of 19 mm and diffuser having the diameter of 40 mm with 180 mm length. the high motive fluid comes out from the nozzle with divergence of expansion angles whenever the nozzle exit position is increase the effect of expansion angles on the entrainment ratio is reduces. So that entrainment ratio increases (Figures 19-22).

Conclusion

In this study CFD technique was employed to investigate the effect of diverging angle of nozzle, NXP and throat of the ejector on the entrainment ratio. Geometry was created in the Ansys 16.0 workbench. The gird elements was initially created in the form of quadrilateral of 140000 elements later it was increased to 180000 elements. This was ensure that the simulation results were independent from the number of grid elements. In this present work, the density-based implicit solver was selected to solve the governing equations which have been proven to be suitable for a supersonic flow field and the flow was set based on steady-state. The convective terms were discredited with a second order upwind scheme. Ideal gas is selected as working fluid in the ejector three cases were analyzed in this work i.e.., NXP, divergent angle of nozzle and throat of ejector, whenever the divergent angle of primary nozzle is increase a series of oblique shocks found in the portion of divergent section. Generally the primary steam will leave the nozzle with some divergence of expansion angle, whenever the divergent angle is increase the divergence of expansion angle will obstruct the flow of secondary inlet so that entrainment ratio decreases in the second case ejector throat was varied, it shows that the whenever the throat of ejector is decrease Because the mixture of primary fluid and secondary fluid will not accelerate to pass through the throat so that incoming secondary mass flow rate to the mixing chamber is reduced finally nxp, whenever the nozzle exit position is increase the effect of expansion angles on the entrainment ratio is reduces. So that entrainment ratio increases.

References

1. Chunnanond K, Aphornratana S (2004) Ejectors: Applications in refrigeration tech-nology. Renew Sustain Energy Rev 8: 129-155.

2. Eames W, Aphornratana S, Haider H (1995) A theoretical and experimental study of a small-scale steam jet refrigerator. Int J Refrigerat 18: 378-386.
3. Aphornratana S, Eames IW (1997) A small capacity steam-ejector refrigerator:experimental investigation of a system using ejector with movable primarynozzle. Int J Refrigerat 20: 352-358.
4. Natthawut R, Satha A, Thanarath S (2011) Experimental studies of a steam jet refrigeration cycle: Effect of the primary nozzle geometries to system performance. Experiment Thermal Fluid Sci 35: 676-683.
5. Meyer AJ, Harms TM, Dobson RT (2009) Steam jet ejector cooling powered by waste or solar heat. Renew Energy 34: 297-306.
6. Pollerberg C, Ahmed HA, Dötsch C (2008) Experimental study on the performance of a solar driven steam jet ejector chiller. Energy Conversion Manage 49: 3318-3325.
7. Sriveerakul T, Aphornratana S, Chunnanond K (2007) Performance prediction of steam ejector using computational fluid dynamics: Part 1 Validation of the CFD results. Int J Thermal Sci 46: 812-822.
8. Sriveerakul T, Aphornratana S, Chunnanond K (2007) Performance prediction of steam ejector using computational fluid dynamics: Part 2 Flow structure of a steam ejector influenced by operating pressures and geometries. Int J Thermal Sci 46: 823-833.
9. Pianthong K, Seehanam W, Behnia M, Sriveerakul T, Aphornratana S (2007) Investigation and improvement of ejector refrigeration system using computational fluid dynamics technique. Energy Conversion Manage 48: 2556-2564.
10. Zhu Y, Cai W, Wen C, Li Y (2009) Numerical investigation of geometry parameters for design of high performance ejectors. Appl Thermal Eng 29: 898-905.
11. Szabolcs V, Oliveira CA, Xiaoli M, Omer SA, Zhang W, et al. (2011) Experimental and numerical analysis of a variable area ratio steam ejector. Int J Refrigerat.
12. Bartosiewicz Y, Aidoun Z, Desevaux P, Mercadier Y (2005) Numerical and experimental investigations on supersonic ejectors. Int J Heat Fluid Flow 26: 56-70.
13. Fan J, Eves J, Thompson HM, Toropov VV, Kapur N, et al. (2011) Computational fluid dynamic analysis and design optimization of jet pumps, Computers & Fluids 46 (1) (July 2011) 212e217.
14. Wang DX, Dong JL (2010) Numerical study on the performances of steam - Jet vacuum pump at different operating conditions. Vacuum 84: 1341-1346.
15. Myoung KJ, Utomo T, Woo J, Lee Y, Jeong H, et al. (2010) CFD investigation on the flow structure inside thermo vapor compressor. Energy 35: 2694-2702.
16. Fluent S (2017) Fluent 6.3 User's guide. Fluent Inc, Lebanon, NH, USA.
17. Cengel YA, Boles MA (2007) Thermodynamics: An Engineering Approach. (6th edn), McGraw-Hill, USA.
18. Yunus A, John MC (2010) Cimbala, fluid mechanics fundamentals and applications. (2nd edn), McGraw-Hill, USA.